Directional Field Computation for Fingerprints Based on the Principal Component Analysis of Local Gradients

Asker M. Bazen and Sabih H. Gerez

University of Twente, Department of Electrical Engineering,
Laboratory of Signals and Systems,
P.O. box 217 - 7500 AE Enschede - The Netherlands
Phone: +31 53 489 3827 Fax: +31 53 489 1060
E-mail: a.m.bazen@el.utwente.nl

Abstract— **This paper discusses a new method, based on the principal component analysis, to estimate the directional field of fingerprints. The method not only computes the direction in any pixel location, but its coherence as well. It will be proven that this method provides exactly the same results as the method that is known from literature. Undoubtedly, the existence of a completely different solution method increases the insight into the problem's nature. Segmentation of fingerprints is discussed to illustrate the application of the coherence of the directional field.**

Keywords— **image processing, fingerprint recognition, orientation estimation, principal component analysis.**

Fig. 1. Example of a fingerprint. The ridges are black and the valleys are white in this figure.

I. Introduction

As can be seen from Figure 1, a fingerprint is built from *ridge-valley* structures. In this figure, the ridges are black and the valleys are white. When using fingerprints for recognition systems, the ridge-valley structures are the main source for the information to be extracted from the fingerprints. It is possible to identify two levels of detail in a fingerprint.

- The *directional field* describes the coarse structure, or basic shape, of a fingerprint. The directional field is defined as the local orientation of the ridge-valley structures. The directional field is for instance used for *classification* of fingerprints.
- The *minutiae* provide the details of the ridge-valley structures, like ridge-endings and bifurcations. Minutiae are for instance used for *matching*, which is a one-to-one comparison of two fingerprints.

A number of approaches to estimate the directional field from a fingerprint is known from literature. Examples are matched-filter methods to find a distinct number of orientations in a fingerprint image [1], [2] and 2-dimensional spectral estimation methods [1]. However, these approaches do not provide as much accuracy as the *gradient-based* methods. The gradient vector $[G_x(x,y)\ G_y(x,y)]^T$ is defined as:

$$\begin{bmatrix} G_x(x,y) \\ G_y(x,y) \end{bmatrix} = \nabla I(x,y) = \begin{bmatrix} \frac{\partial I(x,y)}{\partial x} \\ \frac{\partial I(x,y)}{\partial y} \end{bmatrix} \qquad (1)$$

where $I(x,y)$ represents the gray-scale image. The notion of gradients can best be explained when the pixel values are regarded to indicate height in a continuous 2-dimensional landscape. In this case, the gradient vector is the vector that points in the direction of the steepest descent and the length of the gradient vector is a measure for the steepness [3]. Gradients can be considered as elementary orientations at each pixel of the image.

The directional field is, in principle, perpendicular to the gradients. However, the gradients are orientations at pixel-scale, while the directional field describes the orientation of the ridge-valley structures, which is a much coarser scale. Therefore, the directional field can be derived from the gradients by performing some *averaging* operation on the gradients, involving pixels in some neighborhood [4]. This averaging is the central issue of this paper. Figure 2(a) shows the gradients in a part of a fingerprint, while Figure 2(b) shows the averaged directional field.

This paper is organized as follows. First, in Section II, the traditional method for estimation of the directional field from the gradients is discussed. This method is based on averaging squared gradients. Then, in Section III, a new PCA-based method is proposed. This method provides an analysis of the 2-dimensional joint probability density function of the gradient vectors. In Section IV, a proof is given that that both methods are exactly equivalent. Besides, it is shown that the *coherence*, which is a measure for the local

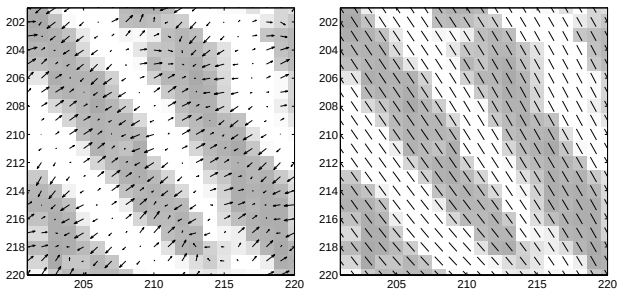

(a) Gradients (b) Directional field

Fig. 2. Detailed area in a fingerprint, (a) shows the gradients and (b) the averaged directional field.

strength of the directional field, can be elegantly expressed in the two eigenvalues, resulting from PCA. In Section V, experimental results in which the coherence is successfully used for segmentation of fingerprints are presented. Finally, in Section VI, the conclusions of this paper are given.

II. Averaging Squared Gradients

This section discusses the problems that are encountered when averaging gradients and the traditional solution of averaging squared gradients. First, the general idea behind averaging squared gradients is presented and then, an analysis of the results of this method is given. Besides the estimation of the directional field, this section also discusses the coherence, which provides a measure for the strength of the estimated orientation.

A. Qualitative analysis

Gradients cannot simply be averaged in some local neighborhood, since opposite gradient vectors will then cancel each other, although they indicate the same ridge-valley orientation. This is caused by the fact that local ridge-valley structures remain unchanged when rotated over 180 degrees [5]. Since the gradient orientations are distributed in a cyclic space ranging from 0 to π and the average orientation has to be found, another formulation of this problem is that the 'π-periodic cyclic mean' has to be computed.

A solution to this problem is to double the angles of the gradient vectors before averaging. After doubling the angles, opposite gradient vectors will point in the same direction and therefore will reinforce each other while perpendicular gradients will cancel. After averaging, the gradient vectors have to be converted back to their single-angle representation. The main ridge-valley orientation is then perpendicular to the direction of the average gradient vector. This method was proposed by [6] and was adopted in some way for the estimation of the directional field of fingerprints by e.g. [7], [8], [9].

In the version of algorithm discussed in this paper, not only the angle of the gradients is doubled, but also the length of the gradient vectors is squared, as if the gradient vectors are considered complex numbers that are squared. This has the effect that strong orientations have a higher vote in the average orientation than weaker orientations. Furthermore, this approach results in the cleanest expressions. However, other choices, like for instance setting all lengths to identity [5], are found in literature as well.

In [6] also a method is proposed to use the squared gradients for computation of the strength of the orientation. This measure, which is called the coherence, measures how well all squared gradient vectors share the same orientation. If they are all parallel, the coherence is 1 and if they are equally distributed over all directions, the coherence is 0.

B. Quantitative Analysis

In this subsection, the qualitative analysis that was given in the previous subsection is made quantitative. The gradient vectors are first estimated in the Cartesian system, in which a gradient vector is given by $[G_x\ G_y]^T$. For the purpose of doubling the angle and squaring the length, the gradient vector is converted to the polar system, in which it is given by $[\rho\ \varphi]^T$, where $-\frac{1}{2}\pi < \phi \leq \frac{1}{2}\pi$. This conversion is given by:

$$\begin{bmatrix} \rho \\ \varphi \end{bmatrix} = \begin{bmatrix} \sqrt{G_x^2 + G_y^2} \\ \tan^{-1} G_y/G_x \end{bmatrix} \tag{2}$$

The gradient vector is converted back to its Cartesian representation by:

$$\begin{bmatrix} G_x \\ G_y \end{bmatrix} = \begin{bmatrix} \rho\cos\varphi \\ \rho\sin\varphi \end{bmatrix} \tag{3}$$

Using some trigonometric identities, an expression for the squared gradient vectors $[G_{s,x}, G_{s,y}]^T$ that makes no use of ρ and φ is found:

$$\begin{aligned} \begin{bmatrix} G_{s,x} \\ G_{s,y} \end{bmatrix} &= \begin{bmatrix} \rho^2\cos 2\varphi \\ \rho^2\sin 2\varphi \end{bmatrix} = \begin{bmatrix} \rho^2(\cos^2\varphi - \sin^2\varphi) \\ \rho^2(2\sin\varphi\cos\varphi) \end{bmatrix} \\ &= \begin{bmatrix} \rho^2[(\frac{G_x}{\rho})^2 - (\frac{G_y}{\rho})^2] \\ \rho^2[2(\frac{G_x}{\rho})(\frac{G_y}{\rho})] \end{bmatrix} = \begin{bmatrix} G_x^2 - G_y^2 \\ 2G_xG_y \end{bmatrix} \end{aligned} \tag{4}$$

This result can also be obtained directly by using the equivalence of 'doubling the angle and squaring the length of a vector' to 'squaring a complex number':

$$G_{s,x} + j\cdot G_{s,y} = (G_x + j\cdot G_y)^2 = (G_x^2 - G_y^2) + j\cdot(2G_xG_y) \tag{5}$$

Now, the average squared gradient $[\overline{G_{s,x}}\ \overline{G_{s,y}}]^T$ can be calculated. It is averaged in some neighborhood, possibly using a non-uniform window W and averaged in the Cartesian plane, which means in x and y:

$$\begin{aligned} \begin{bmatrix} \overline{G_{s,x}} \\ \overline{G_{s,y}} \end{bmatrix} &= \begin{bmatrix} \sum_W G_{s,x} \\ \sum_W G_{s,y} \end{bmatrix} = \begin{bmatrix} \sum_W G_x^2 - G_y^2 \\ \sum_W 2G_xG_y \end{bmatrix} \\ &= \begin{bmatrix} G_{xx} - G_{yy} \\ 2G_{xy} \end{bmatrix} \end{aligned} \tag{6}$$

where

$$G_{xx} = \sum_W G_x^2 \quad (7)$$

$$G_{yy} = \sum_W G_y^2 \quad (8)$$

$$G_{xy} = \sum_W G_x G_y \quad (9)$$

are estimates for the variances and crosscovariance of G_x and G_y, averaged over the window W. Now, the average gradient direction Φ, with $-\frac{1}{2}\pi < \Phi \leq \frac{1}{2}\pi$, is given by:

$$\Phi = \frac{1}{2}\angle\left(G_{xx} - G_{yy}, 2G_{xy}\right) \quad (10)$$

where $\angle(x, y)$ is defined as:

$$\angle(x,y) = \begin{cases} \tan^{-1}(y/x) & x \geq 0 \\ \tan^{-1}(y/x) + \pi \quad \text{for} & x < 0 \wedge y \geq 0 \\ \tan^{-1}(y/x) - \pi & x < 0 \wedge y < 0 \end{cases} \quad (11)$$

and the average ridge-valley direction θ, with $-\frac{1}{2}\pi < \theta \leq \frac{1}{2}\pi$, is perpendicular to Φ:

$$\theta = \begin{cases} \Phi + \frac{1}{2}\pi \quad \text{for} & \Phi \leq 0 \\ \Phi - \frac{1}{2}\pi & \Phi > 0 \end{cases} \quad (12)$$

The coherence of the squared gradients can also be expressed using the same notations. The coherence *Coh* is given by [6]:

$$Coh = \frac{|\sum_W (G_{s,x}, G_{s,y})|}{\sum_W |(G_{s,x}, G_{s,y})|} \quad (13)$$

If all squared gradient vectors are pointing in exactly the same direction, the sum of the moduli of the vectors equals the modulus of the sum of the vectors, resulting in a coherence value of 1. On the other hand, if the squared gradient vectors are equally distributed in all directions, the length of the sum of the vectors will equal 0, resulting in a coherence value of 0. In between these two extreme situations, the coherence will vary between 0 and 1, thus providing the required measure.

III. Principal Component Analysis

This paper proposes a second method to estimate the directional field from the gradients, which is based on *principal component analysis* (PCA). PCA computes a new orthogonal base given a multi-dimensional data set such that the variance of the projections on the axes of this new base is subsequently maximized. It turns out that the base is formed by the eigenvectors of the autocovariance matrix of this data set [10].

Applying PCA to the autocovariance matrix of the $[G_x \;\; G_y]^T$ gradient vectors provides the 2-dimensional Gaussian joint probability density function of these vectors. From this function, the main direction of the gradients can be calculated.

The estimate of the autocovariance matrix $\boldsymbol{C}_G$ of the gradient vector pairs is given by:

$$\boldsymbol{C}_G = \begin{bmatrix} G_{xx} & G_{xy} \\ G_{xy} & G_{yy} \end{bmatrix} = \sum_W \begin{bmatrix} G_x^2 & G_x G_y \\ G_x G_y & G_y^2 \end{bmatrix} \quad (14)$$

In this estimate, the assumption is made that the gradient vectors are zero-mean:

$$E[G_x] = E[G_y] = 0 \quad (15)$$

in a window W in the given fingerprint. This has the effect of first, for each existing gradient vector, creating an additional vector that is mirrored with respect to the origin. Then, the autocovariance matrix is estimated. Because of this procedure, always a zero mean probability density function is estimated, even if the gradients are not zero mean. A zero-mean gradient distribution is a reasonable assumption if the window contains more than one ridge-valley transition.

The longest axis $\boldsymbol{v}_1$ of the 2-dimensional joint probability density function is given by the eigenvector of the autocovariance matrix that corresponds to the largest eigenvalue λ_1. This axis corresponds to the direction in which the variance of the gradients is largest, and so to the 'average' gradient orientation. The ridge-valley orientations are perpendicular to this axis, and therefore given by the shortest axis $\boldsymbol{v}_2$. This is the direction of the eigenvector that corresponds to the smallest eigenvalue λ_2.

The normalized orientation vector $\boldsymbol{v}_n$ is now given by:

$$\boldsymbol{v}_n = \frac{\boldsymbol{v}_1}{|\boldsymbol{v}_1|} \quad (16)$$

The average ridge-valley orientation θ is given by:

$$\theta = \angle \boldsymbol{v}_1 \quad (17)$$

The strength *Str* of the orientation can be defined as a simple function of the two eigenvalues. In order to limit the strength between 0 and 1, it is given by:

$$Str = \frac{\lambda_1 - \lambda_2}{\lambda_1 + \lambda_2} \quad (18)$$

IV. Comparison

In this section, first a comparison will be made between the two methods of directional field estimation. Proof will be given that that both methods are exactly equivalent. Furthermore, in the second part of this section, it will be shown that the coherence *Coh* and strength *Str* are exactly equivalent as well. In the last part of this section, the computational complexity of both methods is compared.

A. Directional field

When comparing the directional fields of a fingerprint, obtained by both methods, at first glance no differences can be seen. It will be proven that both methods are indeed exactly equivalent. The proof starts by deriving the inverse of Equation 4, which was given to be:

$$\begin{bmatrix} G_{s,x} \\ G_{s,y} \end{bmatrix} = \begin{bmatrix} G_x^2 - G_y^2 \\ 2G_xG_y \end{bmatrix} \quad (19)$$

Substituting the lower part of this expression,

$$G_y = \frac{G_{s,y}}{2G_x} \quad (20)$$

into the upper part

$$G_{s,x} = (G_x^2 - G_y^2) \quad (21)$$

gives

$$G_x^4 - G_{s,x}G_x^2 - \frac{1}{4}G_{s,y}^2 = 0 \quad (22)$$

Solving this for G_x gives:

$$G_x = \begin{cases} \frac{1}{2}\sqrt{2G_{s,x} + 2\sqrt{G_{s,x}^2 + G_{s,y}^2}} \\ -\frac{1}{2}\sqrt{2G_{s,x} + 2\sqrt{G_{s,x}^2 + G_{s,y}^2}} \\ \frac{1}{2}\sqrt{2G_{s,x} - 2\sqrt{G_{s,x}^2 + G_{s,y}^2}} \\ -\frac{1}{2}\sqrt{2G_{s,x} - 2\sqrt{G_{s,x}^2 + G_{s,y}^2}} \end{cases} \quad (23)$$

Since φ is restricted to be between $-\frac{1}{2}\pi$ and $\frac{1}{2}\pi$, G_x should always be positive. Therefore, the second and fourth solutions can be eliminated. Furthermore, since $|G_s| \geq G_{s,x}$, the third solution results in the square root of a negative number. Therefore, only the first solution is valid:

$$G_x = \frac{1}{2}\sqrt{2G_{s,x} + 2\sqrt{G_{s,x}^2 + G_{s,y}^2}} \quad (24)$$

The next step is to consider the squared gradients, averaged over the window W and to substitute, according to Equation 6:

$$\overline{G_{s,x}} = G_{xx} - G_{yy} \quad (25)$$

$$\overline{G_{s,y}} = 2G_{xy} \quad (26)$$

The average gradients, derived from the averaged squared gradients, are:

$$\overline{G_x} = \sqrt{\frac{1}{2}(G_{xx} - G_{yy}) + \frac{1}{2}\sqrt{H_{xy}}} \quad (27)$$

and

$$\overline{G_y} = \frac{\overline{G_{s,y}}}{2\overline{G_x}} = \frac{G_{xy}}{\overline{G_x}} = \frac{G_{xy}}{\sqrt{\frac{1}{2}(G_{xx} - G_{yy}) + \frac{1}{2}\sqrt{H_{xy}}}} \quad (28)$$

where, as used in the rest of this text,

$$H_{xy} = (G_{xx} - G_{yy})^2 + 4G_{xy}^2 \quad (29)$$

Now, it can be shown that the vector

$$\begin{bmatrix} \overline{G_x} \\ \overline{G_y} \end{bmatrix} = c \cdot \begin{bmatrix} \frac{1}{2}(G_{xx} - G_{yy}) + \frac{1}{2}\sqrt{H_{xy}} \\ G_{xy} \end{bmatrix} \quad (30)$$

with

$$c = \sqrt{\frac{1}{2}(G_{xx} - G_{yy}) + \frac{1}{2}\sqrt{H_{xy}}} \quad (31)$$

is an eigenvector of $\boldsymbol{C}_G$. This will prove that both methods provide the same results. If this vector is indeed an eigenvector of $\boldsymbol{C}_G$, the following expression must hold:

$$\boldsymbol{C}_G \cdot \boldsymbol{V} = \boldsymbol{V} \cdot \boldsymbol{\Lambda} \quad (32)$$

where the columns of $\boldsymbol{V}$ are the eigenvectors of $\boldsymbol{C}_G$ and $\boldsymbol{\Lambda}$ is the diagonal matrix of the corresponding eigenvalues. This expression must also hold for one eigenvector $\boldsymbol{v}_1$ with corresponding eigenvalue λ_1:

$$\boldsymbol{C}_G \cdot \boldsymbol{v}_1 = \lambda_1 \cdot \boldsymbol{v}_1 \quad (33)$$

Substituting the $[\overline{G_x}\ \overline{G_y}]^T$, ignoring the factor c, for $\boldsymbol{v}_1$ in the left-hand side of this expression gives:

$$\boldsymbol{C}_G \cdot \boldsymbol{v}_1 = \begin{bmatrix} G_{xx} & G_{xy} \\ G_{xy} & G_{yy} \end{bmatrix} \cdot \begin{bmatrix} \frac{1}{2}(G_{xx} - G_{yy}) + \frac{1}{2}\sqrt{H_{xy}} \\ G_{xy} \end{bmatrix} = \begin{bmatrix} G_{xx}\left(\frac{1}{2}(G_{xx} - G_{yy}) + \frac{1}{2}\sqrt{H_{xy}}\right) + G_{xy}^2 \\ G_{xy}\left(\frac{1}{2}(G_{xx} - G_{yy}) + \frac{1}{2}\sqrt{H_{xy}}\right) + G_{xy}G_{yy} \end{bmatrix} \quad (34)$$

Calculating λ_1 from the upper half of these expressions, we find:

$$\lambda_1 = \frac{G_{xx}\left(\frac{1}{2}(G_{xx} - G_{yy}) + \frac{1}{2}\sqrt{H_{xy}}\right) + G_{xy}^2}{\frac{1}{2}(G_{xx} - G_{yy}) + \frac{1}{2}\sqrt{H_{xy}}} \quad (35)$$

which, by multiplying numerator and denominator by $\frac{1}{2}(G_{xx} - G_{yy}) - \frac{1}{2}\sqrt{H_{xy}}$, can be simplified to:

$$\lambda_1 = \frac{1}{2}(G_{xx} + G_{yy}) + \frac{1}{2}\sqrt{H_{xy}} \quad (36)$$

From the lower half of these expressions we find:

$$\lambda_1 = \frac{G_{xy}\left(\frac{1}{2}(G_{xx} - G_{yy}) + \frac{1}{2}\sqrt{H_{xy}}\right) + G_{xy}G_{yy}}{G_{xy}} \quad (37)$$

which can be easily simplified to:

$$\lambda_1 = \frac{1}{2}(G_{xx} + G_{yy}) + \frac{1}{2}\sqrt{H_{xy}} \quad (38)$$

Since both expressions give the same result for λ_1, $\boldsymbol{v}_1$ is an eigenvector of $\boldsymbol{C}_G$. Therefore, both methods are exactly equivalent.

An alternative proof of the equivalence of both methods can be given by using a direct symbolic derivation of the eigenvectors and eigenvalues of $\boldsymbol{C}_G$. The eigenvectors are found to be:

$$\boldsymbol{v}_1 = \begin{bmatrix} \frac{1}{2}(G_{xx} - G_{yy}) + \frac{1}{2}\sqrt{H_{xy}} \\ G_{xy} \end{bmatrix} \quad (39)$$

$$\boldsymbol{v}_2 = \begin{bmatrix} \frac{1}{2}(G_{xx} - G_{yy}) - \frac{1}{2}\sqrt{H_{xy}} \\ G_{xy} \end{bmatrix} \quad (40)$$

Now, it is obvious that:

$$\boldsymbol{v}_1 = c \cdot \begin{bmatrix} \overline{G_x} \\ \overline{G_y} \end{bmatrix} \quad (41)$$

which indicates that $[G_x\ G_y]^T$ is indeed an eigenvector of $\boldsymbol{C}_G$. The eigenvalues are also calculated directly:

$$\lambda_1 = \frac{1}{2}(G_{xx} + G_{yy}) + \frac{1}{2}\sqrt{H_{xy}} \quad (42)$$

$$\lambda_2 = \frac{1}{2}(G_{xx} + G_{yy}) - \frac{1}{2}\sqrt{H_{xy}} \quad (43)$$

Again, the first eigenvalue λ_1 agrees to the already derived eigenvalue.

B. Coherence

In this section, it will be proven that also the coherence *Coh*, calculated using the squared gradient method (see Equation 13) and the strength *Str* (see Equation 18) are exactly equal.

Str is given by:

$$\begin{aligned} Str &= \frac{\lambda_1 - \lambda_2}{\lambda_1 + \lambda_2} \quad (44) \\ &= \frac{\sqrt{(G_{xx} - G_{yy})^2 + 4G_{xy}^2}}{G_{xx} + G_{yy}} \end{aligned}$$

Coh is given by:

$$Coh = \frac{|\sum_W (G_{s,x}, G_{s,y})|}{\sum_W |(G_{s,x}, G_{s,y})|} \quad (45)$$

where

$$\begin{aligned} |\textstyle\sum_W (G_{s,x}, G_{s,y})| &= \sqrt{\left(\sum_W G_{s,x}\right)^2 + \left(\sum_W G_{s,x}\right)^2} \\ &= \sqrt{\left(\sum_W G_x^2 - G_y^2\right)^2 + \left(\sum_W 2G_xG_y\right)^2} \quad (46) \\ &= \sqrt{(G_{xx} - G_{yy})^2 + 4G_{xy}^2} \end{aligned}$$

and

$$\begin{aligned} \sum_W |(G_{s,x}, G_{s,y})| &= \sum_W \sqrt{G_{s,x}^2 + G_{s,y}^2} \\ &= \sum_W \sqrt{(G_x^2 - G_y^2)^2 + (2G_xG_y)^2} \\ &= \sum_W \sqrt{G_x^4 + 2G_x^2G_y^2 + G_y^4} \quad (47) \\ &= \sum_W \sqrt{(G_x^2 + G_y^2)^2} \\ &= \sum_W G_x^2 + G_y^2 \\ &= G_{xx} + G_{yy} \end{aligned}$$

Therefore, the coherence of the averaging method is given by:

$$Coh = \frac{\sqrt{(G_{xx} - G_{yy})^2 + 4G_{xy}^2}}{G_{xx} + G_{yy}} \quad (48)$$

which proves the equivalence of *Coh* and *Str*.

C. Computational Complexity

For efficient calculation of the directional field and the coherence, one should not use one of the two basic methods. Instead, one should use the direct calculations, as given by Expressions 7 to 9, 40 and 48. On a Pentium II 350 MHz computer, calculation of the directional field and the coherence takes approximately 0.5 seconds of processing time for a fingerprint of 300 by 300 pixels.

V. Application to Fingerprints

In this section, an example will be presented in which the previously derived results are applied to fingerprints. This enables the estimation of very accurate and high-resolution directional fields. Furthermore, the coherence is shown to provide correct segmentation results for very noisy fingerprint images.

A. Directional Field Estimation

Most authors process fingerprints blockwise [7], [2]. This means that the directional field is not calculated for all pixels individually. Instead, the average directional field is calculated in blocks of for instance 16×16 pixels. In this section, it will be shown that the processing can be carried out pixelwise, leading to a high resolution and accurate directional field estimate.

In Figure 3(b), an estimate of the directional field is shown. Although the directional field is only shown at discrete steps, it is estimated for each pixel as can be seen from the zoomed Figure 2(b) and from the gray-scale coded Figure 3(c). In this figure, the angles in the range $-\frac{1}{2}\pi$ to $\frac{1}{2}\pi$ have uniformly been mapped to the gray-scales from black to white. This last figure seems to be very chaotic. However, this is only true in the areas that consist of noise. It cannot be seen in this figure that the coherence is very low in noisy areas. Furthermore, it is more important that in the fingerprint area, the figure shows a very smooth directional field.

The directional field is estimated in a number of steps. First, the fingerprint image is low-pass filtered for noise suppression. Then the gradients are estimated. Finally,

(a) Fingerprint (b) Directional field (c) Gray-scale coded directional field

Fig. 3. Original fingerprint, superimposed directional field and gray-scale coded directional field.

the gradients are averaged as described in Section II. This averaging uses a Gaussian window W with $\sigma = 4$.

The estimation method that is described in this paper, enables the application of directional field-related tasks that require very high resolution and accurate directional fields. Examples of these demanding techniques are for instance the accurate extraction of the singular points and obtaining a detailed description of the basic shape of the fingerprint to use for classification or registration of two prints.

B. Coherence-Based Segmentation

The segmentation algorithm separates the foreground of an image from the background. The foreground is the region of interest, containing the fingerprint. The background contains no fingerprint area, but it may contain noise. The processing steps that follow the segmentation expect that the fingerprint is segmented well. That means that they expect a smooth closed area that does not contain much noise.

In noise-free images, the local variance and contrast can be used as a measure for segmentation. Since this can be obtained by simple algorithms, most systems use a blockwise variance-based segmentation measure [8]. However, such systems cannot deal with noisy fingerprint images. When applying a variance-based segmentation method to the fingerprint in Figure 3(a), the "cloud" of noise at the right will also be classified as part of the fingerprint. However, the segmentation method that is proposed here, is capable of successfully identifying areas with noise.

In a fingerprint image, the main distinction between foreground and background is the strength of the orientation of the ridge-valley structures. Therefore, the coherence can be used very well as segmentation criterion. However, even when using using blockwise coherence to segment the fingerprint of Figure 3(a), the main part of the noise will be miss-classified. A segmentation algorithm that is based on the pixelwise coherence, combined with some morphological operations, is capable of accurately segmenting fingerprints of very bad quality that cannot be processed by the variance-based methods.

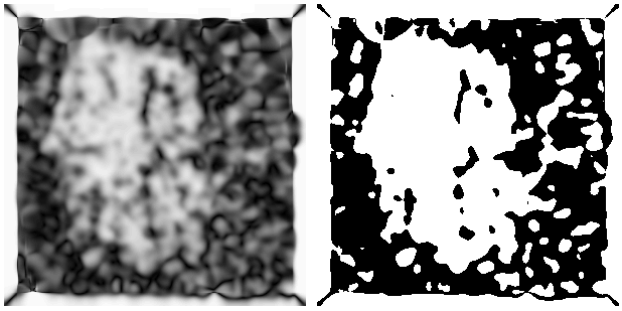

(a) Coherence (b) Thresholded Coherence

Fig. 4. Coherence of the fingerprint of Figure 3(a) and thresholded coherence. In this figure, white indicates 1 and black indicates 0.

Figure 4(a) shows the coherence estimate of the fingerprint from Figure 3(a), estimated using a Gaussian window. It can be clearly seen that in the fingerprint area, the coherence is close to 1, while in the noise area, it is closer to 0. Figure 4(b) shows the result of applying an appropriate threshold to the coherence estimate. It is clear that this mask cannot directly be used for segmentation.

In this mask, a lot of 'noise', can be identified. These spurious points are caused by oriented noise structures and noisy parts in the fingerprint area, which leads to missed and false detections of fingerprint area. In order to remove this from the mask, and get a smooth closed fingerprint area, morphological operations are applied to the mask. As illustrated in Figure 5, first the mask is *opened* [3]. This operation has the effect that small foreground areas are removed. Then, the mask is *closed*, which causes holes in the foreground to be filled. The final segmentation mask is

(a) After opening (b) After closing

Fig. 5. Morphology applied to coherence estimate of Figure 4.

(a) Easy Print (b) Difficult Print

Fig. 6. Segmented fingerprints.

shown in Figure 5(b).

The final result of the segmentation is shown in Figure 6. Not only the noise-free fingerprint of Figure 6(a) is segmented correctly, but also the very noisy fingerprint of Figure 6(b), for which segmentation is a difficult task.

VI. Conclusions

In this paper, a new PCA-based method to estimate directional field from fingerprints is proposed. Since it is proven that this method provides exactly the same results as the traditional method, the method offers a different view and an increase of insight on the problem of estimating an 'average' gradient.

The coherence offers an alternative algorithm for the segmentation of fingerprints. Application of the proposed method to fingerprints shows high resolution and accuracy, compared to the traditional blockwise processing schemes. It is shown that our method is capable of correctly segmenting very noisy fingerprints.

Acknowledgement

This research has been carried out within the *Euregio Computational Intelligence Center* (ECIC), subsidized by the European Commission, The Netherlands and Nordrhein-Westfalen, in the scope of the Interreg Program.

References

[1] C.L. Wilson, G.T. Candela, and C.I. Watson, "Neural network fingerprint classification," *J. Artificial Neural Networks*, vol. 1, no. 2, pp. 203–228, 1994.

[2] K. Karu and A.K. Jain, "Fingerprint classification," *Pattern Recognition*, vol. 29, no. 3, pp. 389–404, 1996.

[3] F. v.d. Heijden, *Image Based Measurement Systems*, John Wiley & Sons Ltd., Chichester, 1994.

[4] T. Lindeberg, *Scale-Space Theory in Computer Vision*, Kluwer Academic Publishers, Boston, 1994.

[5] P. Perona, "Orientation diffusions," *IEEE Transactions On Image Processing*, vol. 7, no. 3, pp. 457–467, Mar. 1998.

[6] M. Kass and A. Witkin, "Analyzing oriented patterns," *Computer Vision, Graphics, and Image Processing*, vol. 37, no. 3, pp. 362–385, Mar. 1987.

[7] A.K. Jain, L. Hong, S. Pankanti, and R. Bolle, "An identity-authentication system using fingerprints," *Proc. of the IEEE*, vol. 85, no. 9, pp. 1365–1388, Sept. 1997.

[8] N. Ratha, S. Chen, and A. Jain, "Adaptive flow orientation based feature extraction in fingerprint images," *Pattern Recognition*, vol. 28, pp. 1657–1672, Nov. 1995.

[9] S.O. Novikov and G.N. Glushchenko, "Fingerprint ridge structure generation models," in *Proceedings of the SPIE, The International Society for Optical Engineering*, 1998, vol. 3346, pp. 270–274.

[10] C.W. Therrien, *Discrete Random Signals and Statistical Signal Processing*, Prentice-Hall, Upper Saddle River, NJ 07458, USA, 1992.